Detonation Wave Structure for Chain-branching Kinetics

Zhe Liang and Luc Bauwens
University of Calgary, Calgary, Alberta, Canada

Corresponding author: Z. Liang (liangz@ucalgary.ca)

Introduction

Combustion kinetics typically include chain-branching. Short and Quirk (1997) performed a linear stability study of detonation waves using a three-step chain-branching model, consisting of a chain-initiation step and a chain-branching step, both governed by Arrhenius kinetics, followed by a pressure and temperature-independent chain-termination step. While that model contains the essential chain-branching dynamics, it only yields one explosion limit, similar to the first or third limit for hydrogen. Based on chain-branching theory of Dainton (1956) and Williams (1985), Liang and Bauwens (2005) considered two pressure-dependent termination steps, yielding the explosion peninsula between first and second limit characteristic of hydrogen. A slightly revised four-step model exhibits an explosion peninsula with three limits. Heat release is associated with termination only. As with the previous model of Liang and Bauwens (2005), Schlieren-type instantaneous images of the field generated from numerical simulation show distinct keystone-shaped regions, associated with substantial differences in reactivity across the shear layer, consistent with experiments in hydrogen-oxygen-argon (Pintgen et al., 2003).

In the high activation energy limit, a steady detonation wave approaches a square-wave profile, consisting of a chemically frozen shock wave followed by an induction period where the reaction rate is still vanishingly small and terminated by a thin fire zone. An empirical square wave model was studied by Zaidel (1961), assuming that no heat generation within an induction zone of specified length. Buckmaster and Neves (1987) presented an asymptotic formulation of the one-dimensional stability problem in the limit of high activation energy, which also led to a leading order square wave model, but formally obtained as a proper limit process. A model assuming (1) high activation energy and (2) very slow initiation allows for resolution of the wave structure and closed form evaluation of the reaction length. Three cases are identified, respectively with post-shock pressure and temperature located (1) within the so-called explosion region; (2) close to the explosion limit; (3) within the no-explosion region. As expected, the reaction length varies very quickly when the post-shock state is close to the explosion limit. In all cases, the chain-branching zone has a structure similar to the single step model of Buckmaster and Ludford (1987). The reaction lengths predicted by the theory are close to numerical results. Numerical simulations show different cell structures and differences in regularity in different zones.

Model

The flow is described by the inviscid, nonconducting reactive Euler equations. The dimensionless conservation equations are

$$\frac{d\rho}{dt} + \rho \boldsymbol{\nabla} \cdot \mathbf{u} = 0, \quad \rho \frac{d\mathbf{u}}{dt} + \boldsymbol{\nabla} \cdot p = 0, \quad \frac{de}{dt} + p \frac{d\rho^{-1}}{dt} = 0 \tag{1}$$

$$\frac{d\lambda_1}{dt} = -r_I - r_B, \quad \frac{d\lambda_2}{dt} = r_I + r_B - r_T \tag{2}$$

where $\mathrm{D}/\mathrm{D}t = \partial/\partial t + \mathbf{u} \cdot \boldsymbol{\nabla}$. Variables ρ, $\mathbf{u}$, p and e are the density, velocity, pressure, total energy respectively. Dimensional scales are chosen with respect to the pre-shock states, such as $\tilde{\rho}_0$ for density, $\tilde{p}_0$ for pressure, $\tilde{T}_0$ for temperature and sound speed $\tilde{c}_0$ for velocity. The time and length scales are defined by the chemistry.

The global chain-branching reaction is represented by four main stages: initiation, chain-branching, wall termination and gas termination. λ_1 is the mass fraction for the reactant and λ_2 the mass fraction for the chain carrier, with

$$r_I = \lambda_1 K_I \exp(-E_I/T), \quad r_B = \rho \lambda_1 \lambda_2 K_B \exp(-E_B/T), \quad r_T = \lambda_2 (K_W + K_G) \tag{3}$$

K_I and K_B are defined by $K_I = \exp(E_I/T_I)$ and $K_B = \exp(E_B/T_B)$, as in Short and Quirk (1997). E_I and E_B are the initiation and chain-branching activation energy respectively. T_I and T_B represent the respective cross-over temperatures at which the chain-initiation and chain-branching rates become as fast as the chain-termination rate at the Neumann point. The wall termination K_W and gas termination K_G are temperature independent, but pressure dependent. K_W is inversely proportional to pressure and K_G is proportional to the square of pressure (Dainton, 1956).

$$K_W = p_{ref}/2p, \quad K_G = (p/p_{ref})^2/[\sigma(p/p_{ref})^2 + 2] \tag{4}$$

where p_{ref} is a reference pressure, setting the time scale. σ is a constant, which was taken to be 0 in Liang and Bauwens (2005). Here $0 < \sigma << 1$.

We assume the fluid is an ideal gas with constant specific heats,

$$e = \frac{p}{(\gamma - 1)\rho} + \frac{1}{2}\mathbf{u} \cdot \mathbf{u} - (1 - \lambda_1 - \lambda_2)Q, \quad p = \rho T \tag{5}$$

where $Q > 0$ represents the total chemical heat release. γ is the ratio of the specific heats.

In a chain-branching reaction, while small, the mass fraction λ_2 of the chain-branching radical initially experiences an exponential growth, because its rate law is of the form $\mathrm{d}\lambda_2/\mathrm{d}t = \lambda_2 F(p, T, ...)$ (the so-called chain-branching explosion). Eventually, however, as its concentration grows larger, termination, which has an exponentially decreasing effect, results in the mass fraction λ_2 reaching a maximum, before disappearing. However, for such a scenario to take place requires that initially, the chain-branching rate must be larger than termination, otherwise any chain-branching radical produced by initiation is directly converted into products and the chain-branching explosion does not take place. Thus the coefficient of λ_2 on the right hand side of Equation 2b must initially be positive.

$$\frac{1}{a} = \frac{r_W(p) + r_G(p)}{r_B(p, T)} = \frac{0.5\left\{p_c/p + (p/p_c)^2/[0.5\sigma(p/p_c)^2 + 1]\right\}}{p/T\lambda_1 \exp[E_B(1/T_B - 1/T)]} \leq 1 \tag{6}$$

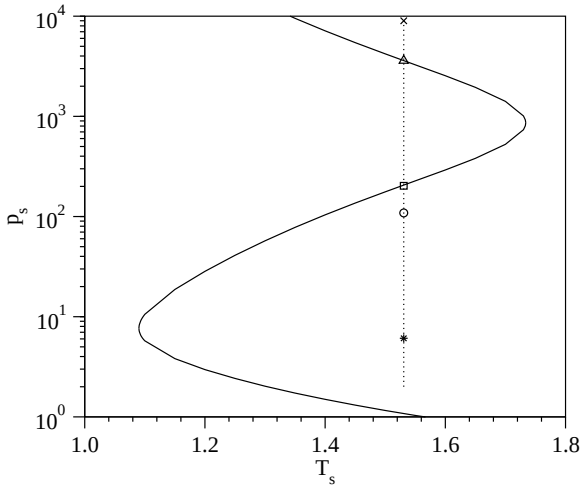

Figure 1: Explosion peninsula behavior of a chain-branching explosion; increasing p_0, p_s moves up along the dotted line; star denotes the point for $p_s/p_{ref} = 1$.

Liang & Bauwens (2005) considered a model equivalent to Equation 4 with sigma=0. They showed that at a given temperature, pressure always has one negative root, which is of no physical significance, and two positive roots, corresponding to two limits. But when $0 < \sigma << 1$, Equation 6 has either three or one positive roots depending upon temperature. The curve $a = 1$ shown in Figure 1 in the p, T plane now exhibits three limits for $E_I = 30$, $E_B = 12$, $T_I = 4.6$, $T_B = 1.3$, $p_{ref} = 6.09$ and $\sigma = 0.0001$. For a heat release $Q = 4$ and an overdrive $f = 1.2$, the post-shock pressure equals p_{ref}. The explosion region lies on the right side of the curve. The lower branch of the curve corresponds to the first limit, due to wall termination, and the two upper ones are the second and third limits, due to gas recombination. At low pressure, $1/p$ is large and the wall termination r_W dominates. As pressure reaches order unity, both wall termination and gas termination are of the same order. As pressure increases to order $O(1/\sqrt{\sigma})$, the gas termination, of $O(1/\sigma)$, dominates. Finally as pressure continues increasing, r_G decreases again to order unity and becomes pressure independent.

If the heat release is maintained constant, then when increasing the pre-shock pressure p_0 but maintaining the pre-shock temperature T_0 constant, the detonation velocity D and the post-shock temperature T_s stay constant. The post-shock pressure p_s moves along the dotted line in Figure 1, crossing between the explosion and non-explosion regions. In this process, the reaction length suffers significant changes because, as seen below, the reaction rate varies significantly.

Reaction Length

We now focus upon the steady planar wave. In Equation 2b, taking into account that the rates are given by Equations 3 and 4, first it is clear that in the absence of initiation, no reaction will ever take place. Furthermore, initiation does not exhibit the potential for exponential growth characteristic of chain-branching. Finally, it is not until termination -the only step taken to be exothermic- will lead to a significant temperature increase that the

temperature-dependence of the initiation rate will play a role. Under these conditions, it is found that the initiation rate is typically quite small.

Likewise, although this may not be quite as realistic, activation energy is taken to be large in the current analysis. The high activation energy model has been quite successful in revealing the structure for single step kinetics (Buckmaster and Neves, 1987) and the same hypothesis is necessary in the current context. The inverse activation energy, denoted by $\beta = T_s/E_B$, is taken to be small. Immediately following the shock wave is the induction zone where all variables ρ, u, p, T, λ_1 and λ_2 are expanded in a form consisting of $O(\beta)$ deviations from the post-shock state,

$$F = F_s + \beta F^{(1)} + O(\beta^2), \quad \beta \ll 1 \tag{7}$$

A length scale is introduced such that the final chain-branching zone has length of order unity, specifically as the scale x_c:

$$x_c = \frac{u_s}{K_W(p_s) + K_G(p_s)} \tag{8}$$

where $K(p_s)$ represents the termination rate at the post-shock pressure. Introducing these expansions into Equations 1 and 2, and collecting in powers of β, two independent equations are obtained at order β:

$$\frac{d{\lambda_2}^{(1)}}{dx} = \epsilon \exp\left(\frac{E_I}{E_B}\theta\right) + (a \exp\theta - 1)\,{\lambda_2}^{(1)}, \quad \frac{d\theta}{dx} = \kappa {\lambda_2}^{(1)} \tag{9}$$

with

$$\theta = \frac{T^{(1)}}{T_s}, \quad \kappa = \frac{1 - \gamma {M_s}^2}{\gamma T_s (1 - {M_s}^2)}(\gamma - 1)Q$$

where ϵ and a defined below characterize the initiation and chain-branching behavior respectively.

$$\epsilon = \frac{K_I/\beta}{K_W(p_s) + K_G(p_s)} \exp\frac{-E_I}{\beta E_B}, \quad a = \frac{\rho_s K_B}{K_W(p_s) + K_G(p_s)} \exp\frac{-1}{\beta}$$

One readily verifies that on the explosion diagram shown in Figure 1, the limit curve is the locus of $a = 1$. When the pre-shock state moves along the dotted fixed temperature line ($T_s = 1.53$) in Figure 1, a equals unity at the chain-branching limits (the point at square or triangle); it is great than 1 in the explosion region (such as the point at star, circle or cross) and less then 1 in the no-explosion region (between square and triangle). In contrast, ϵ remains very small, in a range from 10^{-5} to 10^{-9}.

In Equation 9, initially, ${\lambda_2}^{(1)}$ and $\theta = 0$. If $\epsilon = 0$, the solution remains identically zero and no reaction ever takes place. In all cases, it is thus the first term, of $O(\epsilon)$, on the right hand side of Equation 9 a, that provides initiation, with both $\lambda_2^{(1)}$ and $\theta = O(\epsilon)$. The second term includes the effect of chain-branching, which is temperature-dependent and contributes to an increase in the chin-branching radical, and the effect of termination which is constant in the perturbation equation and consumes the radical, for $a > 1$, this second term results

in a net, increasing, contribution. If $a < 1$, however, it results in a net consumption of chain-branching radicals, because termination is now stronger.

The analysis leads to very different results in these different scenarios. In the first case, for $a > 1$, the initiation length is of $O(-\log\epsilon)$, while in the latter, the length increases to $O(1/\epsilon)$. Finally, in the intermediate case $a = 1$, the initiation length is of $O(\epsilon^{-1/3})$.

For $a > 1$, in the explosion region, the analysis yields the following expression for the length from the von Neumann point to the location where perturbation quantities blow up, indicating the end of the induction length:

$$L = \frac{1}{a-1}\log\frac{(a-1)^2}{\kappa\epsilon}\lim_{\theta\to 0}\left[\theta\exp\int_\theta^\infty \frac{(a-1)d\theta}{a(\exp\theta-1)-\theta}\right] \tag{10}$$

In the chain-branching zone, the solution is similar to that of [5] for single step kinetics. The final singularity in particular is identical. Therefore the steady structure consists of an initiation zone with length of order unity and a chain-branching zone also with length of order unity, which however match over a length of $O(-\log\epsilon)$, yielding an overall reaction length of that order.

For the second case, $a < 1$, in the non-explosion region, termination is initially stronger than chain-branching. Their net combined effect is to slow down initiation, which consequently takes a long time. Chain-branching will only take a role when $a\exp\theta$, which is initially less than 1, becomes larger than 1 as a result of the slow growth of θ due to consumption by the termination step of the radicals produced by initiation, hence also heat release.

$$L = \frac{1}{\kappa\epsilon}\int_0^{-\log a}\frac{1-a\exp\theta}{\exp(E_I\theta/E_B)}d\theta \tag{11}$$

Therefore the initiation zone has a length of order $O(1/\epsilon)$. As before, the length of the chain-branching is of order unity.

Finally, one can study the case a close to unity, which results in a reaction length of order $1/\epsilon^{1/3}$.

Figure 2 shows the reaction length L from the approximate perturbation method (solid) and the numerical exact (dashed) reaction length (from the shock to the peak of λ_2), for the various regimes encountered when the post-shock pressure moves along the dotted line in Figure 1. Except in the non-explosion region, both solutions are really identical. Any difference reflects the approximate nature of the solution based on the assumption of high activation energy. Between the first and the second limit, L goes from 0.7553 at $p_s/p_{ref} = 1$ (star) to a minimum $L = 0.0815$ at $p_s/p_{ref} = 18$ (circle). In that region, termination becomes stronger as p_s increases, but chain-branching is also stronger because ρ_s increases. Therefore chain-branching remains stronger than termination and a remains > 1. As p_s/p_{ref} further increases, L starts to increase, until reaching the second limit for $p_s/p_{ref} = 33.5$ (square), at which point a small change in p_s/p_{ref} leads to a large increase of L. Crossing into the no explosion zone, where a is always less than 1, termination becomes much stronger than chain-branching. The chain-branching radicals produced by the slow initiation reaction are immediately consumed by termination. It is not until the heat release due to termination raises the temperature to the point where chain-branching finally overcomes termination that significant chemistry finally takes place. Thus initiation is very long but compared with the overall length, the final chain-branching and termination processes take a comparatively

very short time. Overall the reaction becomes extremely stiff and the reaction length is more than four orders of magnitude larger than in the explosion region. Finally, beyond the third limit, reached for $p_s/p_{ref} = 580$ at the third limit (triangle), L decreases again as chain-branching is again stronger than termination.

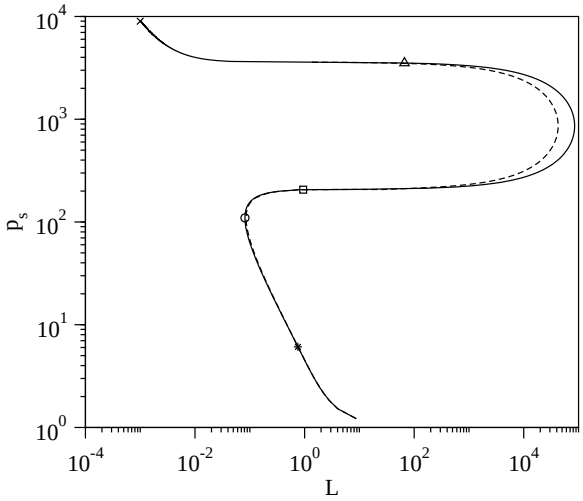

Figure 2: Reaction length L vs. pressure p_s with both the theoretical solution (solid) and the numerical solution (dashed) for p_s/p_{ref} equal to 1 (star), 18 (circle), 33.5 (square), 580 (triangle) and 1500 (cross).

Simulation Results

In our simulations, the reaction zone is captured in a reference frame attached to the wave, hence with inflow and outflow. The initial data consist of the steady profile to which a symmetric sinusoidal disturbance with wavelength equal to the domain width is added in the transverse velocity, immediately behind the shock. Unburnt mixture enters supersonically into the computational domain and burnt mixture exits the domain. An extrapolation relaxes the conditions at exit to the values at infinity.

Figure 3 shows smoke foils for the five cases above: (a) $p_s/p_{ref} = 1$, (b) $p_s/p_{ref} = 10$, (c) $p_s/p_{ref} = 18$, (d) $p_s/p_{ref} = 25$, (e) $p_s/p_{ref} = 30$, in a channel width of 10 $L_{1/2}$. Detonations run from left to right on the smoke foils. In Figure 3 (a), (b) and (c), as p_s/p_{ref} increases from 1 to 18, the reaction length decreases to a minimum. The cell structure changes from regular to irregular. At $p_s/p_{ref} = 18$, one full cell appears initially and develops into half a cell across, eventually changing back to a full cell again. As p_s/p_{ref} increases further between 18 and 25, cells are irregular and switch between one cell and half a cell. When p_s/p_{ref} increases to 25, the cells, shown in (d), become regular again. However, when p_s/p_{ref} approaches the explosion limit curve, the cells are again very irregular. Substructures appear inside cells. For these cases, the ratio between the initiation length and chain-branching length are large, therefore it is very difficult to balance between a reasonable resolution and a computation size. Therefore in order to resolve both the initiation zone and the chain-branching zone, a proper length scale will need to be identified.

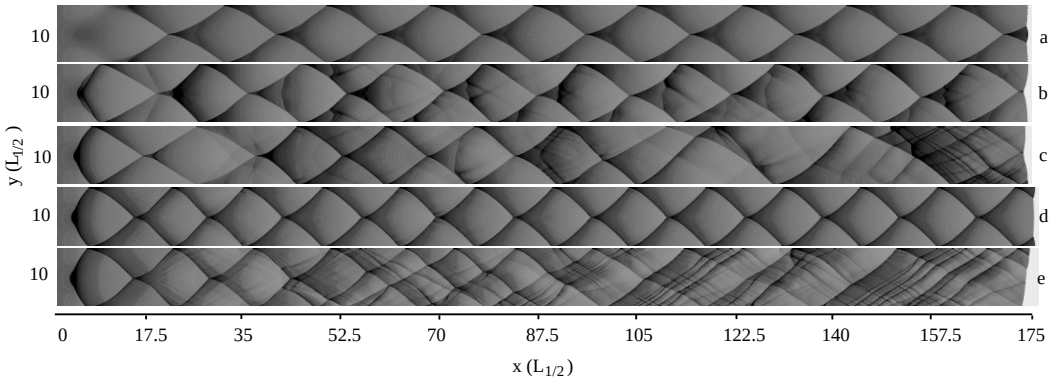

Figure 3: Smoke foils in a channel with width 10 $L_{1/2}$ for p_s/p_{ref} equal to (a) 1, (b) 10, (c) 18, (d) 25 and (e) 30.

Conclusions

A new four-step chain-branching reaction model, consisting of two temperature-dependent Arrhenius steps, chain-initiation and chain-branching, and two pressure-dependent but temperature -independent termination steps, exhibits three explosion limits, similar to hydrogen-oxygen chemistry. A perturbation analysis resolves the steady wave structure, clarifying the differences between different regions and allowing for an evaluation of the reaction length. Comparisons of the reaction length between the theory and the exact numerical integration show that the two solutions are close. Differences result from approximate nature of the assumption of high activation energy. When the chain-branching activation energy is larger, the difference is smaller. The ZND wave structure (not shown in this paper) shows clear square-wave features when the post-shock state is located in the non-explosion region. Numerical smoke foils, performed in a channel width of 10 half reaction length, show that cells become irregular when the reaction length is smaller, and also when the post-shock state is close to the explosion limit.

References

Short M and Quirk J J, 1997, *J. Fluid Mech.* **339**: 89-119.

Dainton F S, 1956, *Chain Reactions, An Introduction.* London: Methuen & Co. Ltd.

Williams F A, 1985, *Combustion Theory* (Menlo Park, VA: Benjamin-Cummings) Appendix B.

Liang Z, Bauwens L, 2005, *Combust. Theory Modelling* **9:1** 93-112.

Pintgen F, Eckett C A, Austin J M & Shepherd J E, 2003 *Combust. Flame*, **133:3** 211-229.

Zaidel, R M, 1961, *Phys. Chem Sect.* **136**: 1142-1145.

Buckmaster J D & Ludford G S S, 1987, *Proc. Combust. Inst.* **21**: 1669-1676.